Published in final edited form as:

J Biomed Mater Res B Appl Biomater. 2018 April ; 106(3): 1258–1267. doi:10.1002/jbm.b.33936.

In vitro evaluation of a basic fibroblast growth factor-containing hydrogel toward vocal fold lamina propria scar treatment

Josh Erndt-Marino[a,#], **Andrea C. Jimenez-Vergara**[a,#], **Patricia Diaz-Rodriguez**[a], **Jonathan Kulwatno**[a], **Juan Felipe Diaz-Quiroz**[a], **Susan Thibeault**[b], and **Mariah S. Hahn**[a,*]

[a]Department of Biomedical Engineering, Rensselaer Polytechnic Institute, Troy, NY

[b]Department of Surgery, Division of Otolaryngology-Head & Neck Surgery, University of Wisconsin School of Medicine and Public Health, Madison, WI

Abstract

Scarring of the vocal fold lamina propria can lead to debilitating voice disorders that can significantly impair quality of life. The reduced pliability of the scar tissue – which diminishes proper vocal fold vibratory efficiency – results in part from abnormal extracellular matrix (ECM) deposition by vocal fold fibroblasts (VFF) that have taken on a fibrotic phenotype. To address this issue, bioactive materials containing cytokines and/or growth factors may provide a platform to transition fibrotic VFF within the scarred tissue toward an anti-fibrotic phenotype, thereby improving the quality of ECM within the scar tissue. However, for such an approach to be most effective, the acute host response resulting from biomaterial insertion/injection likely also needs to be considered. The goal of the present work was to evaluate the anti-fibrotic and anti-inflammatory capacity of an injectable hydrogel containing tethered basic fibroblast growth factor (bFGF) in the dual context of scar and biomaterial-induced acute inflammation. An *in vitro* co-culture system was utilized containing both activated, fibrotic VFF and activated, pro-inflammatory macrophages (MΦ) within a 3D poly(ethylene glycol) diacrylate (PEGDA) hydrogel containing tethered bFGF. Following 72 hours of culture, alterations in VFF and macrophage phenotype were evaluated relative to mono-culture and co-culture controls. In our co-culture system, bFGF reduced the production of fibrotic markers collagen type I, α smooth muscle actin, and biglycan by activated VFF and promoted wound-healing/anti-inflammatory marker expression in activated MΦ. Cumulatively, these data indicate that bFGF-containing hydrogels warrant further investigation for the treatment of the scarred vocal fold.

Keywords

vocal fold lamina propria; vocal fold scar; immunomodulation; basic fibroblast growth factor; 3D cell culture

[*]Corresponding Author: Mariah S. Hahn, PhD, Professor, Biomedical Engineering, Rensselaer Polytechnic Institute, Tel: 518-276-2236, hahnm@rpi.edu.
[#]These authors contributed equally to this work.

1. INTRODUCTION

Scarring of the vocal fold lamina propria (LP) can result in voice changes ranging from hoarseness to complete voice loss depending on the severity of the scar.[1–3] In this often debilitating condition, normal LP pliability is impaired by abnormal extracellular matrix (ECM) deposition and its physical volume is reduced.[1] These changes in LP mechanical and physical properties (pliability and volume) affect the vibratory efficiency of the scarred vocal fold, reducing the quality of cycle-to-cycle closure of the paired vocal fold structures.

Chronic LP scarring has proven difficult to treat with current surgical techniques or standard injectable fillers such as collagen and fat.[1,3,4] Researchers are therefore actively exploring alternative treatment routes, including the development of designer biomaterial implants for functional LP regeneration.[5–36] To date, most biomaterials developed for treatment of LP scar have been screened *in vitro* for their capacity to elicit desired ECM production from VFF as the biomaterial degrades prior to *in vivo* evaluation.[27–36] Although this approach has yielded significant advances, it does not capture several aspects of the *in vivo* implant environment which critically impact biomaterial-associated VFF ECM production. For example, the VFF commonly used to assess various biomaterials *in vitro* are generally "normal" or "non-fibrotic".[27–36] However, fibroblasts associated with chronic vocal fold scar display fibrotic/myofibroblastic phenotypes.[37] Furthermore, *in vitro* culture formats that include only VFF do not account for the fact that biomaterials induce an acute inflammatory response upon implantation, leading to macrophage (MΦ) activation.[38–40] This is significant since MΦ phenotype has been shown to strongly impact resident fibroblast ECM production.[41–43] As such, biomaterials intended for treatment of vocal fold scar should be designed not only to transition activated (myofibroblastic) VFF towards a more normal phenotype but also to elicit desired phenotypes from activated, pro-inflammatory MΦ.

To address this challenge, biomaterials containing bioactive factors with anti-fibrotic and/or immunomodulatory functionality could potentially be used for treatment of scarred LP. Indeed, recent studies have investigated the anti-fibrotic influence of dexamethasone and hyaluronic acid on VFF pre-stimulated toward a myofibroblast phenotype.[15,44] Ideally, such biomaterial additives would induce local myofibroblasts to take on a "normal" VFF phenotype and promote pro-inflammatory MΦ to alter their polarization toward an anti-inflammatory/pro-tissue healing phenotype. A growing body of literature indicates that basic fibroblast growth factor (bFGF) has direct anti-fibrotic effects on VFF and indirect anti-inflammatory effects.[8–10,24,35,45–49] Specifically, VFF treated with bFGF have consistently shown reduced expression of α smooth muscle actin (a marker generally associated with a myofibroblast phenotype) and increased expression of MMP-1 and hyaluronic acid synthase 2 (markers generally associated with an anti-fibrotic phenotype).[9,10,46] In addition, bFGF has been shown to increase VFF expression of the anti-inflammatory molecule hepatocyte growth factor (HGF).[9] Despite these generally noted beneficial effects, conflicting reports of bFGF effects on VFF expression of the fibrotic markers collagen types I and III exist,[9,10,24,35,46–49] and bFGF is rapidly absorbed *in vivo*.[50] Because of these limitations, clinical success may require repeated dosing,[51,52] particularly in cases of scarring in older patients.[53] The disruption/damage to the vocal fold LP associated with repeated injections is known to be deleterious to LP tissue and inductive of LP scar. Thus, a biomaterial which can locally

retain therapeutic levels of growth factors such as bFGF for extended periods of time, avoiding repeated intervention, would be desirable.[45]

Poly(ethylene glycol) diacrylate (PEGDA) based hydrogels may be chemically modified with growth factors or cytokines through tethering into the PEGDA network, providing a convenient method for local growth factor retention. Proteins tethered into PEGDA hydrogel networks are effectively inhibited from being internalized by cells.[54,55] This feature allows for repeated signaling by a single bFGF molecule, enabling lower doses to be employed for growth factors like bFGF that do not require cell internalization to effect changes in cell behavior.[56] Furthermore, PEGDA hydrogels degrade hydrolytically over a period of 3 – 6 months,[57] slowly releasing tethered bFGF over this time frame and allowing for new tissue to be deposited as the hydrogel structure degrades. This is in contrast to the release associated with bFGF-loaded gelatin hydrogels previously examined in VFF literature, from which the majority of release occurs within 14 days.[10] Certain PEGDA hydrogel formulations have also previously been shown to permit preservation of the vocal fold mucosal wave with low phonation threshold pressures.[58] Thus, the present work was designed to investigate the influence of a bFGF-containing PEGDA hydrogel on activated VFF phenotype and MΦ polarization in 3D co-culture conditions. This format is significantly different from previous *in vitro* evaluations of bFGF effects on VFF in that it contains activated VFF and activated MΦ. We envision that a liquid precursor solution containing acrylate-derivatized bFGF and PEGDA can be injected into the injured vocal fold LP and subsequently crosslinked into a hydrogel by trans-epithelial light exposure.[59] This hydrogel will then provide localized, extended exposure of the tethered growth factor(s) to the resident VFF and MΦ.

Figure 1 depicts the overall experimental design for the present study. In order to mimic some of the complex conditions characterizing chronic scar and acute inflammation following biomaterial insertion – such as the presence of activated VFF and MΦ – normal, unactivated porcine VFF (VFF^-) and unactivated RAW 264.7 murine MΦ ($M\Phi^-$) were stimulated for 5 days utilizing “activation media” containing lipopolysaccharide (LPS) and transforming growth factor-beta 1 (TGF-β1, Figure 1A). TGF-β1 has been previously been established to induce normal VFF to take on characteristics of a myofibroblast phenotype,[16,37,60] with LPS stimulation potentially exacerbating this effect.[61] Similarly, exogenous delivery of LPS (commonly utilized to induce classical macrophage activation)[38,41,62,63] combined with immunomodulatory TGF-β1 is anticipated based on literature[64] to evoke a pro-inflammatory macrophage phenotype similar to that seen in many biomaterial-treated dermal wounds (loosely, a phenotype between the traditional M1 and M2 classifications).[65,66]

In the present work, this activation protocol was first verified in 2D culture before moving into more complex 3D studies, which utilized activated VFF (VFF^+) and activated MΦ ($M\Phi^+$) encapsulated within biocompatible[67] PEGDA hydrogels containing the cell adhesion ligand RGDS as well as tethered bFGF (Figure 1B). Following encapsulation, VFF^+ and $M\Phi^+$ were cultured within bFGF-containing hydrogels for 72 h in the sustained presence of activation media (LPS/TGF-β1) to continue to mimic some of the complex conditions characterizing chronic scar and acute inflammation following biomaterial insertion.

2. MATERIALS AND METHODS

2.1 Polymer synthesis

PEGDA was prepared as previously described by combining 0.1 mmol mL^{-1} dry PEG (10 kDa, Fluka), 0.4 mmol mL^{-1} acryloyl chloride, and 0.2 mmol mL^{-1} triethylamine in anhydrous dichloromethane with stirring under argon overnight.[68] The resulting solution was washed with 2 M K_2CO_3 and separated into aqueous and dichloromethane phases to remove HCl. The dichloromethane phase was subsequently dried with anhydrous $MgSO_4$, and PEGDA was precipitated in diethyl ether, filtered, and dried under vacuum. The extent of PEG diacrylation was determined by ^1H NMR to be ~95%.

Recombinant human bFGF (17 kDa; 13256-029, Life Technologies) and the cell adhesion peptide RGDS (American Peptide) were reacted with acryloyl-PEG-N-hydroxysuccinimide (ACRL-PEG-SVA) (3.4 kDa, Laysan Bio) at a 1:3 and 1:1 molar ratio, respectively, for 2 h in 50 mM sodium bicarbonate buffer, pH 8.5.[56,69] Recombinant human bFGF has previously been shown to effectively interact with both murine[70] and porcine[71] cells. In addition, bFGF is known to maintain its potency following reaction with an acrylate-derivatized PEG linker and subsequent incorporation within a PEGDA hydrogel.[72] ACRL-PEG-bFGF was purified by dialysis, stored at −20 °C, and used within 24 h of storage. ACRL-PEG-RGDS was purified by dialysis, lyophilized, and stored at −80 °C until use.

2.2 Cell culture

Cryopreserved porcine vocal fold fibroblasts (VFF) at passage 6 were obtained from Robert Langer, ScD (Massachusetts Institute of Technology).[73] These cells had been isolated from primary explants of the mid-membranous LP of 6–12-month-old pigs, an accepted animal model for the human vocal fold LP.[2,64] The discarded animal tissues were obtained from the MIT Division of Comparative Medicine and with the approval of the MIT animal care committee. The cryopreserved VFF were thawed and expanded at 37 °C/5% CO_2 in Dulbecco's Modified Eagle's Medium (DMEM, Cellgro) supplemented with 10 % fetal bovine serum (FBS, Atlanta Biologicals), 2 ng mL^{-1} bFGF (Invitrogen), 100 U mL^{-1} penicillin, and 100 μg mL^{-1} streptomycin (Gibco).

Cryopreserved RAW 264.7 murine MΦ (ATCC) were thawed and expanded in a monolayer culture. Macrophages were maintained at 37 °C/5% CO_2 in maintenance media (DMEM supplemented with 10 % FBS, 100 U mL^{-1} penicillin, and 100 μg mL^{-1} streptomycin).

2.3 Cell activation with LPS/TGF-β1

Prior to encapsulation, VFF and MΦ were cultured for 5 days with either maintenance media [MM: DMEM supplemented with 10 % FBS, 100 U ml^{-1} penicillin, and 100 μg ml^{-1} streptomycin] or activation medium [AM: maintenance media supplemented with 1 μg ml^{-1} LPS from Salmonella enterica serotype enteritidis (Sigma Aldrich) and 5 ng ml^{-1} TGF-β1 (Millipore)]. LPS and TGF-β1 were chosen for use in AM to mimic the complex microenvironment during chronic scar and acute inflammation.[16,19,20,37,41,60] The activation protocol is depicted schematically in Figure 1A.

To confirm changes in cell phenotype resulting from 5 day activation, the phenotype of VFF and MΦ cultured in AM [VFF^+ and $M\Phi^+$, respectively] was compared to that of VFF and MΦ cultured in MM [VFF^- and $M\Phi^-$]. Specifically, mRNA was isolated from $M\Phi^+$ and $M\Phi^-$ (n = 4 per treatment group) using Dynabeads mRNA direct kit (Life Technologies). In brief, kit lysis buffer was added to culture wells containing $M\Phi^+$ or $M\Phi^-$ and incubated for 10 min. After the incubation period, polyA-mRNA was isolated from each cell lysate using 20 μL of Dynabeads oligo $(dT)_{25}$ magnetic beads. Following rinsing steps, the polyA-mRNA was released from the Dynabeads in 100 μL of 10 mM Tris-HCl by heating the beads to 80 °C for 2 min. Remaining cell lysate (containing DNA and proteins) was collected and stored at −20 °C for subsequent DNA and protein analyses. Protein lysates of VFF^+ and VFF^- (n = 4 per treatment group) were similarly prepared.

2.4 Hydrogel fabrication and maintenance

Hydrogels were fabricated by first preparing a precursor solution containing 100 mg mL^{-1} 10 kDa PEGDA and 1 mM ACRL-PEG-RGDS in phosphate-buffered saline (PBS, Gibco). PEGDA molecular weight and concentration were selected to yield hydrogels with average dynamic elastic moduli appropriate to vocal fold applications.[27,74] The concentration of RGDS was chosen based on previous work with VFF.[16,34] Photoinitiator solution (262 mg mL^{-1} in 70% ethanol) was then added at 1 vol% to the precursor solution, after which the it was passed through using a 0.2 μm Acrodisc® Filter Unit with a Mustang® E membrane (Pall Life Science) for the purpose of sterilization and endotoxin removal. For hydrogels including bFGF, sterile and endotoxin-free ACRL-PEG-bFGF solution was then added to the precursor solution to achieve a bFGF concentration of 100 ng ml^{-1}. This concentration was chosen based off of previous *in vitro* studies which demonstrated a therapeutic benefit with soluble bFGF at 100 ng ml^{-1}.[9,10]

VFF and/or macrophages that had been cultured for 5 days in AM were harvested and resuspended in the various precursor solutions, each at ~$1x10^6$ cells ml^{-1}. Two hundred μl of the resulting suspensions were pipetted into a 48 well plate and polymerized by 6 min exposure to longwave UV light (Spectroline, ~6 mW cm^{-2}, 365 nm). Six different experimental groups were prepared as shown in Figure 1B. Polymerized hydrogels were transferred to BD Falcon culture inserts (12 mm diameter, 0.8 μm pores) and immersed in AM. After 24 h of culture at 37 °C/5% CO_2, a set of hydrogel discs was selected for mechanical analyses. Fresh AM was added to each remaining hydrogel disc and the gels were cultured for an additional 48 h.

2.5 Rheological testing

Punches (8mm in diameter) were prepared from the hydrogel discs harvested at 24 h and were used to characterize the rheological behavior of the PEGDA network. Hydrogels were blotted gently to remove excess media and were placed on the testing stage of an Anton-Paar Physica MCR 301 rheometer fitted with an 8 mm diameter upper platen. The gap distance between the upper and lower platen was adjusted to achieve a 100 μm indentation depth within each hydrogel. Dynamic oscillatory frequency sweeps were then conducted at room temperature between 0.1 Hz and 30 Hz, with 10 measurement points per decade at a constant shear stress of 2%. The PEGDA formulation utilized herein (10%, 10 kDa)

displayed an average shear storage modulus of ~10.7 ± 0.2 kPa and a damping ratio of ~0.45 at 30 Hz (Supplementary Figure 1). These results are consistent with the shear storage modulus and damping ratio values of ~8 kPa and 0.55, respectively, previously reported for 10% 10 kDa PEGDA hydrogels at 40 Hz.[34] Shear storage modulus and damping ratio ranges for the native vocal fold LP at similar strains and loading frequencies are 0.1–7 kPa and 0.6–2, respectively.[75,76]

2.6 Endpoint analyses

Following 72 h of culture, hydrogels were transferred to 1.7 mL RNase-free conical tubes, flash frozen in liquid nitrogen, and stored at −80 °C for subsequent gene and protein analyses.

2.6.1 Gene expression

mRNA isolation: mRNA was extracted using Dynabeads mRNA direct kit (Life Technologies). In brief, the hydrogels were placed in contact with 300 μL of lysis binding buffer. The samples were then homogenized using a plastic RNase free pestle (Kimble Chase) and incubated at room temperature for 15 min. Following incubation, the samples were centrifuged for 5 min at 10,000 rpm and the polyA-mRNA in the supernatant was extracted using 20 μL of Dynabeads oligo $(dT)_{25}$ magnetic beads. To improve the yield of extraction, a second round of polyA-mRNA extraction was performed. The mRNA-laden Dynabeads were rinsed and transferred to 100 μL of a 10 mM Tris-HCl buffer, into which the bound polyA-mRNA was released by heating the beads to 80 ºC for 2 min. The mRNA solution was then stored at −80 ºC until further analysis. Remaining sample homogenate was collected and stored at −20 °C for subsequent DNA measurement and protein analyses.

Quantitative RT-PCR (qRT-PCR): Hydrogels containing macrophages were analyzed for expression of various markers associated with classically-activated, wound healing, or anti-inflammatory macrophage phenotypes. Verified qRT-PCR primers for mouse inducible nitric oxide synthase (iNOS), tumor necrosis factor (TNF), subunit beta of interleukin 12 (IL-12β), interleukin-1 beta (IL-1β), arginase-1 (Arg-1), vascular endothelial growth factor (VEGF), interleukin-10 (IL-10), chitinase-3 like protein 3 (Chi3l3), and glyceraldehyde 3-phosphate dehydrogenase (GAPDH) were obtained from Origene or Operon. Primer sequences are provided in Table 1. A StepOne real time PCR system (Life Technologies) and the SuperScript III Platinum One-Step qRT-PCR kit (Life Technologies) were utilized for the gene expression analyses. At least 3 samples were assessed by qRT-PCR for each experimental group, with each sample being evaluated in duplicate for each gene. Approximately 3 ng of polyA-mRNA and 5 μL of 1 μM primer were added per 25 μL of reaction mixture. Amplification during the PCR phase was monitored by measuring the change in SYBR Green fluorescence using ROX dye as a passive reference. A threshold fluorescence value at which each sample was in the exponential phase of amplification was identified using StepOne software v2.0. The amplification cycle at which a given sample crossed this threshold was recorded as the C_t for that sample. For each sample, the expression of each gene of interest relative to GAPDH was calculated using the $\Delta\Delta C_t$ method. Melting temperature analysis was performed for each PCR reaction to verify the appropriate amplification product. The associated melting temperatures are reported in Table

1. Given the presence of porcine VFF in the VFF/MΦ co-culture samples, the selectivity of each mouse primer for the associated mouse mRNA was confirmed as detailed in Supplementary Table 1.

2.6.2 DNA Assessment—Briefly, DNA levels in sample homogenates from the mRNA extraction process were measured using the Quant-iT™ PicoGreen dsDNA Assay (Life Technologies). Sample volumes representing equal amounts of DNA (750 ng) were concentrated using 3000 MWCO Amicon filter units (Millipore) for western blot analyses.

2.6.3 Western blot—Changes in VFF phenotype following 72 h of encapsulation were semi-quantitatively evaluated for each VFF-containing hydrogel via western blot analysis. Antibodies for collagen type I (Col 1; clone NB600-448, Millipore), α smooth muscle actin (αSMA; clone 1A4, Santa Cruz Biotechnology), and biglycan (clone ab49701, Abcam) - proteins generally associated with a fibrotic/myofibroblastic VFF phenotype[9,10,16,44] - were examined. In addition, an antibody targeting the matrix metalloproteinase-1 (MMP-1; clone N-17, SCBT) – a protein generally considered as anti-fibrotic[77] – was utilized. An antibody for the reference protein GAPDH (clone 6F7, Santa Cruz Biotechnology) was utilized as a normalizer.

Samples containing equal amounts of DNA (750 ng for VFF per lane) were treated with β-mercaptoethanol, heated at 95 °C for 10 min, and then loaded into a 10 or 12% polyacrylamide gel. Sample proteins were separated by electrophoresis and subsequently transferred to a nitrocellulose membrane (Thermo Scientific). After protein transfer, the membrane was blocked with a 5% BSA solution (Fraction V, Fisher Scientific) in Tris-buffered saline containing 0.1% Tween-20 (TBST; 25 mM Tris-HCl, pH. 7.5, 137 mM NaCl, 0.1% Tween 20) for 1 h at room temperature. Primary antibodies were diluted in TBST containing 5% BSA and applied to the membranes overnight at 4 °C with constant rotation. Bound primary antibodies were detected by the application of appropriate horseradish peroxidase-conjugated or alkaline phosphatase-conjugated secondary antibody (Jackson ImmunoResearch) for 1 h at room temperature, followed by the application of Luminol (Santa Cruz Biotechnology) or Novex chemiluminescent substrate (Life Technologies), respectively, for the development of signal. Chemiluminescence was detected using a ChemiDoc™ XRS+ System equipped with Image Lab™ Software (Bio-Rad Laboratories), with exposure time controlled to avoid signal saturation. For each protein, band integrated optical density was quantified using Adobe Photoshop.

Each target protein was then normalized to the corresponding levels of GAPDH. Given the presence of mouse macrophage proteins in the VFF/MΦ co-culture samples, antibody specificity for porcine proteins was confirmed utilizing mouse 3T3 control samples (Supplementary Figure 2).

2.7 Statistical analyses

Data are reported as mean ± standard deviation. Comparisons of sample means were performed by one-way ANOVA or MANOVA, as appropriate. Homogeneity of variances was confirmed with Levene's test and Box's test for ANOVA and MANOVA analysis,

respectively. Tukey's post hoc test (SPSS software) was utilized when there were more than 2 experimental groups (n = 3–8 samples per group), $p < 0.05$.

3. RESULTS

3.1 Verifying cell activation in 2D culture

As shown schematically in Figure 1, normal VFF (VFF^{-}) and unactivated MΦ ($M\Phi^{-}$) were stimulated for 5 days utilizing "activation media" containing LPS and TGF-β1. This stimulation regimen was intended to induce VFF^{-} to take on a myofibroblast-like phenotype (VFF^{+}) typical of scarred LP[16,37,60] and $M\Phi^{-}$ to take on a pro-inflammatory macrophage phenotype ($M\Phi^{+}$) similar to that seen in dermal wounds treated with RGD-containing PEGDA hydrogels (loosely, a phenotype between the traditional M1 and M2 classifications).[65,66] Using these activated cells, we could subsequently assess the ability of the bFGF-containing hydrogels to shift this fibrotic VFF phenotype and initial "M1/M2" macrophage phenotype toward more anti-fibrotic and pro-healing phenotypes, respectively.

Prior to encapsulating these activated cells within PEGDA hydrogels, the activation state of the VFF^{+} and $M\Phi^{+}$ was confirmed. Supplementary Figure 3 shows the production of αSMA, biglycan, Col 1, and fibronectin – markers generally associated with a VFF myofibroblast phenotype[9,10,16,44] – by VFF^{+} relative to VFF^{-} as evaluated by western blot. As anticipated based on previous work with VFF,[16,37,60,61] there was an overall increase in the production of several myofibroblast markers by VFF^{+} relative to VFF^{-} ($p = 0.001$; Supplementary Figure 3). Similarly, Figure 2 shows the relative gene expression of several markers associated with the diverse range of macrophage activation states by $M\Phi^{+}$ relative to $M\Phi^{-}$. Specifically, markers traditionally associated with the M1 (classically-activated) phenotype and the M2 phenotype (including both wound healing and anti-inflammatory markers) were assessed (Table 1).

Per these gene expression analyses, $M\Phi^{+}$ cells displayed increased levels of pro-inflammatory iNOS (~2.5 fold, $p = 0.008$) and TNF (~3.7 fold, $p = 0.007$) mRNA relative to $M\Phi^{-}$ (Figure 2). Furthermore, $M\Phi^{+}$ expression levels of the wound healing marker Arg-1 (~68.3 fold, $p < 0.001$) and the anti-inflammatory marker IL-10 (~4.75 fold, $p = 0.001$) were significantly higher than that of $M\Phi^{-}$ (Figure 2). Notably, this LPS/TGF-β1 activation pattern is distinct from LPS treatment alone (Supplementary Figure 4), a commonly utilized method to activate macrophages towards a classically-activated phenotype.[38,62,63] In particular, LPS/TGF-β1 treatment generally resulted in reduced expression of traditional M1 markers and increased expression of M2 markers relative to LPS stimulation alone. Taken together, these data indicate that stimulation of macrophages with LPS/TGF-β1 yielded a macrophage activation pattern with both classically-activated and wound-healing characteristics, as is typical of the MΦ phenotype associated with the acute inflammation seen in dermal wounds treated with RGD-containing PEGDA hydrogels.[66]

3.2 Evaluating cell response to tethered bFGF in 3D culture

Following confirmation of the activation of VFF and MΦ in 2D, VFF^{+} and $M\Phi^{+}$ were encapsulated either alone or together within 3D PEGDA hydrogel discs containing the cell

adhesion ligand RGDS, but either with or without tethered bFGF (Figure 1B). Following 3 days of culture in the continued presence of activation media, the phenotype of encapsulated VFF and MΦ were analyzed via western blot and qRT-PCR, respectively.

3.2.1 VFF phenotype—Figure 3 displays the relative protein levels of Col 1, αSMA, and biglycan – markers generally considered to be fibrotic[9,10,16,44] – produced by: 1) VFF^+ alone in PEGDA hydrogels without bFGF (VFF^+), 2) VFF^+ alone in PEGDA hydrogels containing bFGF (bFGF/VFF^+), 3) VFF^+ in co-culture with $M\Phi^+$ in PEGDA hydrogels without bFGF ($VFF^+/M\Phi^+$), and 4) VFF^+ in co-culture with $M\Phi^+$ in PEGDA hydrogels containing bFGF (bFGF/$VFF^+/M\Phi^+$). In addition, the relative protein levels of MMP-1 – a marker generally considered as anti-fibrotic[77] – across VFF treatment groups are shown. Representative western blot images are provided in Supplementary Figure 5.

As shown in Figure 3, the inclusion bFGF in the bFGF/VFF^+ group resulted in a significant increase in Col 1 production (~1.4 fold, $p = 0.028$) relative to the VFF^+ group, although there was no significant effect of bFGF on the production of αSMA or biglycan. While MMP-1 levels appeared to be increased (~1.5 fold) in the bFGF/VFF^+ group relative to the VFF+ group, this effect also fell below statistical significance ($p = 0.077$). The majority of prior *in vitro* studies assessing VFF response to bFGF have been performed using RT-PCR as the assessment tool. In order to compare our observed bFGF effects to existing VFF literature, we therefore conducted additional gene level analyses of Col 1, Col III, αSMA, and MMP-1 (Supplementary Figure 6). Our qRT-PCR data were found to be consistent with the cumulative results from VFF literature, despite the presence of TGF-β1 in our culture medium.[9,10,24,35,46–49]

The inclusion of activated macrophages in the $VFF^+/M\Phi^+$ group resulted in no significant change in any of the analyzed protein markers relative to the VFF^+ group (Figure 3). However, there was a significant decrease in biglycan production in $VFF^+/M\Phi^+$ relative to bFGF/VFF^+ (~1.5 fold, $p = 0.018$). Several additional differences became apparent with the incorporation of bFGF into hydrogels containing both VFF^+ and $M\Phi^+$. Specifically, in contrast to the increase in Col 1 noted for the bFGF/VFF^+ group relative to the VFF^+ group, there was a marked reduction in Col 1 levels (> 2.3 fold, $p < 0.001$) in the bFGF/$VFF^+/M\Phi^+$ group relative to the VFF^+, bFGF/VFF^+, and $VFF^+/M\Phi^+$ groups (Figure 3). Levels of αSMA were reduced by at least a factor of 1.9 in the bFGF/VFF/$M\Phi^+$ relative to all remaining treatment groups ($p < 0.041$). Biglycan levels were also significantly lower in the bFGF/$VFF^+/M\Phi^+$ group relative to the both the VFF^+ (~2.0 fold, $p = 0.001$) and bFGF/VFF^+ (~2.2 fold, $p < 0.001$) groups. However, while MMP-1 levels were ~1.7-fold lower in the bFGF/$VFF^+/M\Phi^+$ group relative to the bFGF/VFF^+ group ($p = 0.017$), they were unchanged relative to the VFF^+ only group. Cumulatively, these data indicate that bFGF may be capable of reducing VFF production of "pro-fibrotic markers" (Col 1, αSMA, and biglycan) in the dual context of chronic scar and biomaterial-induced macrophage activation (i.e. in $VFF^+/M\Phi^+$ co-culture).

3.2.2 MΦ phenotype—Figure 4 displays the relative gene expression of markers representing the diverse range of MΦ activation in the following treatment groups: 1) $M\Phi^+$ alone in PEGDA hydrogels without bFGF ($M\Phi^+$), 2) $M\Phi^+$ alone in PEGDA hydrogels

containing bFGF (bFGF/MΦ$^+$), 3) MΦ$^+$ in co-culture with VFF$^+$ in PEGDA hydrogels without bFGF (MΦ$^+$/VFF$^+$), and 4) MΦ$^+$ in co-culture with VFF$^+$ in PEGDA hydrogels containing bFGF (bFGF/MΦ$^+$/VFF$^+$). Treatment with bFGF alone appeared to result in minimal shifts in MΦ$^+$ gene expression for all markers examined except for the wound-healing marker Arg-1, which was ~4 fold lower in the bFGF/MΦ$^+$ group relative to the MΦ$^+$ only group ($p = 0.021$). The inclusion of co-culture with VFF$^+$ also appeared to have limited effects on MΦ$^+$ gene expression for most markers examined, with the apparent increase in IL-12β mRNA (~2.8 fold) falling below statistical significance ($p = 0.096$). However, there was a substantial decrease in the mRNA levels of the pro-inflammatory marker iNOS (~3.1 fold, $p = 0.010$) in MΦ$^+$/VFF$^+$ group relative to the MΦ$^+$ group (Figure 4).

In contrast to the influence of bFGF or VFF$^+$ alone on MΦ$^+$ gene expression, MΦ$^+$ treatment with both bFGF and VFF$^+$ resulted in significant shifts in the mRNA levels of several MΦ$^+$ markers. In particular, there were significant decreases in the gene expression of Arg-1 (~3 fold, $p = 0.040$) and IL-12β (~4.7 fold, $p = 0.042$) in bFGF/MΦ$^+$/VFF$^+$ group relative to MΦ$^+$ only group and MΦ$^+$/VFF$^+$ group, respectively. Furthermore, there were marked increases in the mRNA levels of the anti-inflammatory markers IL-10 and Chi3l3 in the bFGF/MΦ$^+$/VFF$^+$ group relative to all other experimental groups ($p < 0.001$, Figure 4). Combined, these data indicate that bFGF appeared to be capable of shifting MΦ$^+$ phenotype toward a more anti-inflammatory phenotype in the dual context of chronic scar and biomaterial-induced macrophage activation (i.e. in MΦ$^+$/VFF$^+$ co-culture).

4. DISCUSSION

In the present study, the capacity of tethered bFGF to transition myofibroblastic/fibrotic VFF towards a “normal” phenotype as well as to elicit a more pro-healing phenotype from activated, pro-inflammatory MΦ was evaluated *in vitro*. We envision that these shifts in phenotype will, over the long-term, improve the quality of VFF ECM deposition within the scarred tissue region and thereby improve overall vocal fold function. To mimic the VFF phenotype characteristic of chronic scarring and the MΦ phenotype characteristic of acute inflammation following PEGDA-RGD hydrogel insertion, “normal” VFF and unactivated MΦ were treated with activation media containing both LPS and TGF-β1 for 5 days prior to encapsulation. VFF treated with activation media displayed an overall increase in the myofibroblast markers assessed relative to untreated VFF, in agreement with established culture models involving VFF exposure to TGF-β1.[16,37,60] In addition, MΦ treated with activation media showed an increase in markers associated with pro-inflammatory activation (iNOS and TNF) as well as wound healing and anti-inflammatory markers (Arg-1 and IL-10, respectively) relative to untreated macrophages. However, LPS/TGF-β1 treatment also generally resulted in reduced expression of traditional M1 markers and increased expression of M2 markers relative to LPS stimulation alone. Taken together, these data indicate that stimulation of macrophages with LPS/TGF-β1 yielded a macrophage activation pattern between classically-activated and wound healing phenotypes. As desired,[78,79] this macrophage phenotype resembled that associated with the acute inflammation following treatment of dermal wounds with RGD-containing PEGDA hydrogels.[66]

After confirming the activation of VFF and MΦ in 2D, these activated cells (VFF^+ and $M\Phi^+$) were encapsulated within 3D PEGDA hydrogels either with or without tethered bFGF. After 3 days of culture in the continued presence of activation media, western blotting revealed that bFGF significantly increased VFF^+ production of the pro-fibrotic marker Col 1, while fibrotic markers αSMA and biglycan remained essentially unchanged relative to the VFF^+ only group. Similarly, VFF^+ exposure to $M\Phi^+$ had minimal impact on VFF^+ phenotype for the markers examined. These data indicate that the effects of bFGF alone or $M\Phi^+$ alone on VFF^+ phenotype appeared to be limited and neither strictly pro- nor anti-fibrotic. The present results are in contrast to the general anti-fibrotic effects of bFGF noted in the literature for VFF. In particular, bFGF has generally been observed to down-regulate Col 1 expression[9,10,35,46] and αSMA production[10] by VFF. The differences between the current results and existing literature could potentially be attributed to several factors (e.g. differences in media formulation, bFGF exposure time, 2D vs. 3D culture, gene versus protein level phenotypic assessment[80]). However, qRT-PCR analyses our bFGF/VFF^+ group versus the VFF^+ only group (Supplementary Figure 6) yielded cumulative results consistent with VFF literature, despite the presence of TGF-β1 in our culture medium.[9,10,24,35,46–49] In particular, bFGF exposure was associated with a ~60% decrease αSMA mRNA and a ~80% increase in MMP-1 mRNA levels.

Interestingly, bFGF appeared to exert a greater influence on VFF^+ behavior when applied to VFF^+ in co-culture with $M\Phi^+$. Notably, VFF^+ in the bFGF/VFF^+/$M\Phi^+$ group produced significantly lower Col 1 than the VFF^+ group and the VFF^+/$M\Phi^+$ group. Furthermore, protein levels of the fibrotic markers αSMA and biglycan – which were unaffected by bFGF in the VFF^+ mono-culture group – were significantly reduced in the bFGF/VFF^+/$M\Phi^+$ group relative to both the VFF^+ group and the bFGF/VFF^+ groups. In contrast, VFF^+ expression of the anti-fibrotic marker MMP-1 in the bFGF/VFF^+/$M\Phi^+$ group remained essentially unchanged relative to the VFF^+ only group. Thus, although tethered bFGF did not have expected protein-level anti-fibrotic effects on VFF^+ in mono-culture, the present co-culture results indicate that bFGF may have net anti-fibrotic effects in the dual context of chronic scar and biomaterial-induced macrophage activation.

To gain insight into potential ways in which bFGF was achieving these effects on VFF^+ phenotype in co-culture, we investigated the activation status of encapsulated $M\Phi^+$ utilizing a panel of markers indicative of pro-inflammatory, anti-inflammatory, and wound healing phenotypes. While the influence of bFGF on macrophage recruitment during wound healing has been well studied,[81,82] literature reports in which macrophages are explicitly stimulated with bFGF are relatively scarce. Therefore, to the authors' knowledge, this is the first report to study macrophage activation with respect to multiple potential phenotypes in response to bFGF stimulation. As for the VFF^+ data, bFGF alone did not appear to exert a strong influence on $M\Phi^+$ phenotype for the markers examined. Indeed, only Arg-1 expression was altered in the bFGF/$M\Phi^+$ group relative to the $M\Phi^+$ group, with the mRNA levels of this wound-healing marker being significantly reduced in bFGF/$M\Phi^+$ group. Similarly, only iNOS expression was significantly impacted by $M\Phi^+$ co-culture with VFF^+ in the absence of bFGF, with mRNA levels of this pro-inflammatory marker being significantly lower in the VFF^+/$M\Phi^+$ group relative to the $M\Phi^+$ group. This reduction in pro-inflammatory marker

expression by $M\Phi^+$ exposed to VFF^+ is consistent with the reduction in pro-inflammatory markers observed for activated macrophages co-cultured with scar VFF.[41]

As for the VFF^+, bFGF appeared to exert a greater influence on $M\Phi^+$ behavior when applied in co-culture. Specifically, the bFGF/$M\Phi^+$/VFF^+ group displayed significantly lower mRNA levels of the pro-inflammatory marker IL-12β and the wound healing marker Arg-1 mRNA relative to the $M\Phi^+$/VFF^+ group and the $M\Phi^+$ group, respectively. In addition, gene expression of the anti-inflammatory markers IL-10 and Chi3l3 were markedly increased in the bFGF/$M\Phi^+$/VFF^+ group relative to all other treatment groups. The implications of the associated decrease in Arg-1 expression noted for the bFGF/MΦ and bFGF/$M\Phi^+$/VFF^+ groups are difficult to interpret as increases in Arg-1 have been linked not only to wound healing but also to fibrosis.[83,84] However, the IL-12β, IL-10, and Chi3l3 data for the bFGF/$M\Phi^+$/VFF^+ group indicate that bFGF may be capable of transitioning $M\Phi^+$ towards a more anti-inflammatory phenotype in the dual context of scar and biomaterial-insertion. This shift in $M\Phi^+$ phenotype in the bFGF/$M\Phi^+$/VFF^+ group may partly underlie the observed anti-fibrotic shift in VFF^+ phenotype in this treatment group. This interpretation would be consistent with a previous study which found that certain anti-inflammatory cytokines can decrease αSMA expression by VFF pre-stimulated with TGF-β1.[60]

Overall, the current results are encouraging and support the primary goal of this study – the initial development of an injectable PEGDA-based hydrogel with tethered bFGF with the potential to reduce/modify chronic LP scar through modulation of VFF and MΦ phenotypes. However, it should be noted that vocal fold LP scar and acute inflammation following biomaterial insertion represent a complex set of processes that are mediated by a number of factors, only a subset of which were captured within the present culture format. Furthermore, while beneficial effects were noticed with the bFGF tethered to the PEGDA network, potential differences in cell response between soluble and tethered growth factors were not investigated. In addition, the use of cells from two separate species (porcine fibroblasts versus mouse macrophages) likely reduced the efficacy of fibroblast-macrophage cross-talk in co-culture. Another potential issue with the current co-culture format is the possibility of heterotypic cell interactions, which render it difficult to definitively state whether the effects were caused by paracrine and/or heterotypic cell-cell interactions.

5. CONCLUSION

We have evaluated the capacity of bFGF tethered within PEGDA hydrogels to reduce the myofibroblastic VFF phenotype associated with vocal fold LP scar utilizing an *in vitro* 3D co-culture system. Activated VFF and MΦ were employed in order to recapitulate key aspects of the complex microenvironment associated with biomaterial-treatment of scarred LP. Interestingly, while the protein level influence of bFGF appeared to be limited in mono-culture, bFGF incorporated in VFF/MΦ co-culture resulted in reduced production of Col 1, αSMA, and biglycan from activated VFF and increased anti-inflammatory cytokine gene expression from activated MΦ. Cumulatively, these results suggest that bFGF-containing PEGDA hydrogels warrant further investigation for the treatment of the scarred vocal fold LP.

Supplementary Material

Refer to Web version on PubMed Central for supplementary material.

Acknowledgments

This work was supported by a grant from the NIH (R01 DC013508) to S.T and M.S.H. The authors thank Dr. Ryan Gilbert for use of his rheometer.

References

1. Dailey SH, Ford CN. Surgical management of sulcus vocalis and vocal fold scarring. Otolaryngologic clinics of North America. 2006; 39(1):23–42. [PubMed: 16469653]
2. Hansen JK, Thibeault SL. Current understanding and review of the literature: vocal fold scarring. Journal of Voice. 2006; 20(1):110–120. [PubMed: 15964741]
3. Graupp M, Bachna-Rotter S, Gerstenberger C, Friedrich G, Fröhlich-Sorger E, Kiesler K, Gugatschka M. The unsolved chapter of vocal fold scars and how tissue engineering could help us solve the problem. European Archives of Oto-Rhino-Laryngology. 2016; 273(9):2279–2284. [PubMed: 26108198]
4. Rosen CA. Phonosurgical vocal fold injection: procedures and materials. Otolaryngologic Clinics of North America. 2000; 33(5):1087–1096. [PubMed: 10984772]
5. Fishman JM, Long J, Gugatschka M, De Coppi P, Hirano S, Hertegard S, Thibeault SL, Birchall MA. Stem cell approaches for vocal fold regeneration. Laryngoscope. 2016; 126(8):1865–1870. [PubMed: 26774977]
6. Kutty JK, Webb K. Mechanomimetic hydrogels for vocal fold lamina propria regeneration. Journal of Biomaterials Science, Polymer Edition. 2009; 20(5–6):737–756. [PubMed: 19323887]
7. Kutty JK, Webb K. Tissue engineering therapies for the vocal fold lamina propria. Tissue Engineering Part B: Reviews. 2009; 15(3):249–262. [PubMed: 19338432]
8. Suehiro A, Hirano S, Kishimoto Y, Rousseau B, Nakamura T, Ito J. Treatment of acute vocal fold scar with local injection of basic fibroblast growth factor: a canine study. Acta otolaryngologica. 2010; 130(7):844–850.
9. Suehiro A, Hirano S, Kishimoto Y, Tateya I, Rousseau B, Ito J. Effects of basic fibroblast growth factor on rat vocal fold fibroblasts. The Annals of otology, rhinology, and laryngology. 2010; 119(10):690–696.
10. Hiwatashi N, Hirano S, Mizuta M, Kobayashi T, Kawai Y, Kanemaru Si, Nakamura T, Ito J, Kawai K, Suzuki S. The efficacy of a novel collagen–gelatin scaffold with basic fibroblast growth factor for the treatment of vocal fold scar. Journal of tissue engineering and regenerative medicine. 2015
11. Coppoolse JM, Van Kooten TG, Heris HK, Mongeau L, Li NY, Thibeault SL, Pitaro J, Akinpelu O, Daniel SJ. An in vivo study of composite microgels based on hyaluronic acid and gelatin for the reconstruction of surgically injured rat vocal folds. J Speech Lang Hear Res. 2014; 57(2):S658–73. [PubMed: 24687141]
12. King SN, Hanson SE, Chen X, Kim J, Hematti P, Thibeault SL. In vitro characterization of macrophage interaction with mesenchymal stromal cell-hyaluronan hydrogel constructs. J Biomed Mater Res A. 2014; 102(3):890–902. [PubMed: 23564555]
13. Tong Z, Duncan RL, Jia X. Modulating the behaviors of mesenchymal stem cells via the combination of high-frequency vibratory stimulations and fibrous scaffolds. Tissue Eng Part A. 2013; 19(15–16):1862–78. [PubMed: 23516973]
14. Tong Z, Sant S, Khademhosseini A, Jia X. Controlling the fibroblastic differentiation of mesenchymal stem cells via the combination of fibrous scaffolds and connective tissue growth factor. Tissue Eng Part A. 2011; 17(21–22):2773–85. [PubMed: 21689062]
15. Kosinski AM, Pothen JM, Panitch A, Sivasankar MP. Dexamethasone Controlled Release on TGF-beta1 Treated Vocal Fold Fibroblasts. Ann Otol Rhinol Laryngol. 2015; 124(7):572–8. [PubMed: 25667215]

16. Kosinski AM, Sivasankar MP, Panitch A. Varying RGD concentration and cell phenotype alters the expression of extracellular matrix genes in vocal fold fibroblasts. J Biomed Mater Res A. 2015; 103(9):3094–100. [PubMed: 25778824]
17. Hiwatashi N, Hirano S, Suzuki R, Kawai Y, Mizuta M, Kishimoto Y, Tateya I, Kanemaru S, Nakamura T, Dezawa M, et al. Comparison of ASCs and BMSCs combined with atelocollagen for vocal fold scar regeneration. Laryngoscope. 2016; 126(5):1143–1150. [PubMed: 26403510]
18. Pitman MJ, Cabin JA, Iacob CE. Small Intestinal Submucosa Implantation for the Possible Treatment of Vocal Fold Scar, Sulcus, and Superficial Lamina Propria Atrophy. Annals of Otology Rhinology and Laryngology. 2016; 125(2):137–144.
19. Valerie A, Vassiliki K, Irini M, Nikolaos P, Karampela E, Apostolos P. Adipose-Derived Mesenchymal Stem Cells in the Regeneration of Vocal Folds: A Study on a Chronic Vocal Fold Scar. Stem Cells International. 2016
20. Shiba TL, Hardy J, Luegmair G, Zhang ZY, Long JL. Tissue-Engineered Vocal Fold Mucosa Implantation in Rabbits. Otolaryngology-Head and Neck Surgery. 2016; 154(4):679–688. [PubMed: 26956198]
21. Li LQ, Teller S, Clifton RJ, Jia XQ, Kiick KL. Tunable Mechanical Stability and Deformation Response of a Resilin-Based Elastomer. Biomacromolecules. 2011; 12(6):2302–2310. [PubMed: 21553895]
22. Fastenberg JH, Roy S, Smith LP. Coblation-assisted management of pediatric airway stenosis. Int J Pediatr Otorhinolaryngol. 2016; 87:213–8. [PubMed: 27368474]
23. Hiwatashi N, Bing R, Kraja I, Branski RC. Mesenchymal stem cells have antifibrotic effects on transforming growth factor-β1-stimulated vocal fold fibroblasts. The Laryngoscope. 2016 n/a–n/a.
24. Suzuki R, Kawai Y, Tsuji T, Hiwatashi N, Kishimoto Y, Tateya I, Nakamura T, Hirano S. Prevention of vocal fold scarring by local application of basic fibroblast growth factor in a rat vocal fold injury model. Laryngoscope. 2016
25. Young WG, Hoffman MR, Koszewski IJ, Whited CW, Ruel BN, Dailey SH. Voice Outcomes following a Single Office-Based Steroid Injection for Vocal Fold Scar. Otolaryngol Head Neck Surg. 2016
26. Luo Y, Kobler JB, Heaton JT, Jia XQ, Zeitels SM, Langer R. Injectable Hyaluronic Acid-Dextran Hydrogels and Effects of Implantation in Ferret Vocal Fold. Journal of Biomedical Materials Research Part B-Applied Biomaterials. 2010; 93B(2):386–393.
27. Liao H, Munoz-Pinto D, Qu X, Hou Y, Grunlan MA, Hahn MS. Influence of hydrogel mechanical properties and mesh size on vocal fold fibroblast extracellular matrix production and phenotype. Acta biomaterialia. 2008; 4(5):1161–1171. [PubMed: 18515199]
28. Chen X, Thibeault SL. Biocompatibility of a synthetic extracellular matrix on immortalized vocal fold fibroblasts in 3-D culture. Acta Biomater. 2010; 6(8):2940–8. [PubMed: 20109588]
29. Kutty JK, Webb K. Vibration stimulates vocal mucosa-like matrix expression by hydrogel-encapsulated fibroblasts. Journal of Tissue Engineering and Regenerative Medicine. 2010; 4(1): 62–72. [PubMed: 19842110]
30. Grieshaber SE, Farran AJE, Lin-Gibson S, Kiick KL, Jia XQ. Synthesis and Characterization of Elastin-Mimetic Hybrid Polymers with Multiblock, Alternating Molecular Architecture and Elastomeric Properties. Macromolecules. 2009; 42(7):2532–2541. [PubMed: 19763157]
31. Farran AJE, Teller SS, Jha AK, Jiao T, Hule RA, Clifton RJ, Pochan DP, Duncan RL, Jia XQ. Effects of Matrix Composition, Microstructure, and Viscoelasticity on the Behaviors of Vocal Fold Fibroblasts Cultured in Three-Dimensional Hydrogel Networks. Tissue Engineering Part A. 2010; 16(4):1247–1261. [PubMed: 20064012]
32. Sahiner N, Jha AK, Nguyen D, Jia XQ. Fabrication and characterization of cross-linkable hydrogel particles based on hyaluronic acid: potential application in vocal fold regeneration. Journal of Biomaterials Science-Polymer Edition. 2008; 19(2):223–243. [PubMed: 18237494]
33. Wolchok JC, Tresco PA. Using Vocally Inspired Mechanical Conditioning to Enhance the Synthesis of a Cell-derived Biomaterial. Annals of Biomedical Engineering. 2013; 41(11):2358–2366. [PubMed: 23793412]

34. Jimenez-Vergara AC, Munoz-Pinto DJ, Becerra-Bayona S, Wang B, Iacob A, Hahn MS. Influence of glycosaminoglycan identity on vocal fold fibroblast behavior. Acta biomaterialia. 2011; 7(11): 3964–3972. [PubMed: 21740987]
35. Hiwatashi N, Hirano S, Mizuta M, Tateya I, Kanemaru S-i, Nakamura T, Ito J, Kawai K, Suzuki S. Biocompatibility and efficacy of collagen/gelatin sponge scaffold with sustained release of basic fibroblast growth factor on vocal fold fibroblasts in 3-dimensional culture. Annals of Otology, Rhinology & Laryngology. 2014 0003489414546396.
36. Munoz-Pinto DJ, Jimenez-Vergara AC, Gelves LM, McMahon RE, Guiza-Arguello V, Hahn MS. Probing vocal fold fibroblast response to hyaluronan in 3D contexts. Biotechnology and bioengineering. 2009; 104(4):821–831. [PubMed: 19718686]
37. Branco A, Bartley SM, King SN, Jette ME, Thibeault SL. Vocal fold myofibroblast profile of scarring. Laryngoscope. 2016; 126(3):E110–7. [PubMed: 26344050]
38. Lynn AD, Bryant SJ. Phenotypic changes in bone marrow-derived murine macrophages cultured on PEG-based hydrogels activated or not by lipopolysaccharide. Acta biomaterialia. 2011; 7(1): 123–132. [PubMed: 20674808]
39. Rodero MP, Khosrotehrani K. Skin wound healing modulation by macrophages. International journal of clinical and experimental pathology. 2010; 3(7):643. [PubMed: 20830235]
40. Bartlett RS, Thibeault SL, Prestwich GD. Therapeutic potential of gel-based injectables for vocal fold regeneration. Biomed Mater. 2012; 7(2):024103. [PubMed: 22456756]
41. King SN, Chen F, Jetté ME, Thibeault SL. Vocal fold fibroblasts immunoregulate activated macrophage phenotype. Cytokine. 2013; 61(1):228–236. [PubMed: 23123198]
42. Lim J-Y, Choi BH, Lee S, Jang YH, Choi J-S, Kim Y-M. Regulation of wound healing by granulocyte-macrophage colony-stimulating factor after vocal fold injury. PloS one. 2013; 8(1):e54256. [PubMed: 23372696]
43. Swartzlander MD, Lynn AD, Blakney AK, Kyriakides TR, Bryant SJ. Understanding the host response to cell-laden poly(ethylene glycol)-based hydrogels. Biomaterials. 2013; 34(4):952–64. [PubMed: 23149012]
44. Chen X, Thibeault SL. Response of fibroblasts to transforming growth factor-beta1 on two-dimensional and in three-dimensional hyaluronan hydrogels. Tissue Eng Part A. 2012; 18(23–24): 2528–38. [PubMed: 22734649]
45. Kobayashi T, Mizuta M, Hiwatashi N, Kishimoto Y, Nakamura T, Kanemaru S-i, Hirano S. Drug delivery system of basic fibroblast growth factor using gelatin hydrogel for restoration of acute vocal fold scar. Auris Nasus Larynx. 2016
46. Shi H-X, Lin C, Lin B-B, Wang Z-G, Zhang H-Y, Wu F-Z, Cheng Y, Xiang L-J, Guo D-J, Luo X. The anti-scar effects of basic fibroblast growth factor on the wound repair in vitro and in vivo. PloS one. 2013; 8(4):e59966. [PubMed: 23565178]
47. Luo Y, Kobler JB, Zeitels SM, Langer R. Effects of growth factors on extracellular matrix production by vocal fold fibroblasts in 3-dimensional culture. Tissue Engineering. 2006; 12(12): 3365–3374. [PubMed: 17518673]
48. Ohno T, Yoo MJ, Swanson ER, Hirano S, Ossoff RH, Rousseau B. Regenerative Effects of Basic Fibroblast Growth Factor on Extracellular Matrix Production in Aged Rat Vocal Folds. Annals of Otology Rhinology and Laryngology. 2009; 118(8):559–564.
49. Song R, Bian HN, Lai W, Chen HD, Zhao KS. Normal skin and hypertrophic scar fibroblasts differentially regulate collagen and fibronectin expression as well as mitochondrial membrane potential in response to basic fibroblast growth factor. Braz J Med Biol Res. 2011; 44(5):402–10. [PubMed: 21445528]
50. Isogai N, Morotomi T, Hayakawa S, Munakata H, Tabata Y, Ikada Y, Kamiishi H. Combined chondrocyte-copolymer implantation with slow release of basic fibroblast growth factor for tissue engineering an auricular cartilage construct. J Biomed Mater Res A. 2005; 74(3):408–18. [PubMed: 15973729]
51. Hirano S, Mizuta M, Kaneko M, Tateya I, Kanemaru S, Ito J. Regenerative phonosurgical treatments for vocal fold scar and sulcus with basic fibroblast growth factor. Laryngoscope. 2013; 123(11):2749–55. [PubMed: 23553343]

52. Ban MJ, Park JH, Kim JW, Park KN, Lee JY, Kim HK, Lee SW. The Efficacy of Fibroblast Growth Factor for the Treatment of Chronic Vocal Fold Scarring: From Animal Model to Clinical Application. Clin Exp Otorhinolaryngol. 2016
53. Kanazawa T, Komazawa D, Indo K, Akagi Y, Lee Y, Nakamura K, Matsushima K, Kunieda C, Misawa K, Nishino H, et al. Single Injection of Basic Fibroblast Growth Factor to Treat Severe Vocal Fold Lesions and Vocal Fold Paralysis. Laryngoscope. 2015; 125(10):E338–E344. [PubMed: 25953726]
54. Mann BK, Schmedlen RH, West JL. Tethered-TGF-beta increases extracellular matrix production of vascular smooth muscle cells. Biomaterials. 2001; 22(5):439–444. [PubMed: 11214754]
55. Saik JE, Gould DJ, Watkins EM, Dickinson ME, West JL. Covalently immobilized platelet-derived growth factor-BB promotes angiogenesis in biomimetic poly(ethylene glycol) hydrogels. Acta Biomaterialia. 7(1):133–143.
56. DeLong SA, Moon JJ, West JL. Covalently immobilized gradients of bFGF on hydrogel scaffolds for directed cell migration. Biomaterials. 2005; 26(16):3227–3234. [PubMed: 15603817]
57. Browning MB, Cereceres SN, Luong PT, Cosgriff-Hernandez EM. Determination of the in vivo degradation mechanism of PEGDA hydrogels. Journal of Biomedical Materials Research Part A. 2014; 102(12):4244–4251. [PubMed: 24464985]
58. Karajanagi SS, Lopez-Guerra G, Park H, Kobler JB, Galindo M, Aanestad J, Mehta DD, Kumai Y, Giordano N, d'Almeida A. Assessment of canine vocal fold function after injection of a new biomaterial designed to treat phonatory mucosal scarring. Annals of Otology, Rhinology & Laryngology. 2011; 120(3):175–184.
59. Elisseeff J, Anseth K, Sims D, McIntosh W, Randolph M, Langer R. Transdermal photopolymerization for minimally invasive implantation. Proceedings of the National Academy of Sciences of the United States of America. 1999; 96(6):3104–3107. [PubMed: 10077644]
60. Vyas B, Ishikawa K, Duflo S, Chen X, Thibeault SL. Inhibitory effects of HGF and IL-6 on TGF-β1 mediated vocal fibroblast-myofibroblast differentiation. The Annals of otology, rhinology, and laryngology. 2010; 119(5):350.
61. King SN, Berchtold CM, Thibeault SL. Lipopolysaccharide responsiveness in vocal fold fibroblasts. J Inflamm (Lond). 2014; 11(1):42. [PubMed: 25606025]
62. Meng F, Lowell CA. Lipopolysaccharide (LPS)-induced macrophage activation and signal transduction in the absence of Src-family kinases Hck, Fgr, and Lyn. The Journal of experimental medicine. 1997; 185(9):1661–1670. [PubMed: 9151903]
63. Amura CR, Kamei T, Ito N, Soares MJ, Morrison DC. Differential regulation of lipopolysaccharide (LPS) activation pathways in mouse macrophages by LPS-binding proteins. The Journal of Immunology. 1998; 161(5):2552–2560. [PubMed: 9725255]
64. King SN, Guille J, Thibeault SL. Characterization of the Leukocyte Response in Acute Vocal Fold Injury. PLoS One. 2015; 10(10):e0139260. [PubMed: 26430970]
65. Witherel CE, Graney PL, Freytes DO, Weingarten MS, Spiller KL. Response of human macrophages to wound matrices in vitro. Wound Repair and Regeneration. 2016; 24(3):514–524. [PubMed: 26874797]
66. Lynn AD, Blakney AK, Kyriakides TR, Bryant SJ. Temporal progression of the host response to implanted poly(ethylene glycol)-based hydrogels. J Biomed Mater Res A. 2011; 96(4):621–31. [PubMed: 21268236]
67. Lynn AD, Kyriakides TR, Bryant SJ. Characterization of the in vitro macrophage response and in vivo host response to poly (ethylene glycol)-based hydrogels. Journal of Biomedical Materials Research Part A. 2010; 93(3):941–953. [PubMed: 19708075]
68. Munoz-Pinto DJ, McMahon RE, Kanzelberger MA, Jimenez-Vergara AC, Grunlan MA, Hahn MS. Inorganic–organic hybrid scaffolds for osteochondral regeneration. Journal of Biomedical Materials Research Part A. 2010; 94(1):112–121. [PubMed: 20128006]
69. Munoz-Pinto DJ, Bulick AS, Hahn MS. Uncoupled investigation of scaffold modulus and mesh size on smooth muscle cell behavior. Journal of Biomedical Materials Research Part A. 2009; 90(1):303–316. [PubMed: 19402139]
70. Elenius K, Maatta A, Salmivirta M, Jalkanen M. Growth factors induce 3T3 cells to express bFGF-binding syndecan. J Biol Chem. 1992; 267(9):6435–41. [PubMed: 1556147]

71. Fujishiro SH, Nakano K, Mizukami Y, Azami T, Arai Y, Matsunari H, Ishino R, Nishimura T, Watanabe M, Abe T, et al. Generation of naive-like porcine-induced pluripotent stem cells capable of contributing to embryonic and fetal development. Stem Cells Dev. 2013; 22(3):473–82. [PubMed: 22889279]
72. DeLong SA, Moon JJ, West JL. Covalently immobilized gradients of bFGF on hydrogel scaffolds for directed cell migration. Biomaterials. 2005; 26(16):3227–34. [PubMed: 15603817]
73. Hahn MS, Teply BA, Stevens MM, Zeitels SM, Langer R. Collagen composite hydrogels for vocal fold lamina propria restoration. Biomaterials. 2006; 27(7):1104–1109. [PubMed: 16154633]
74. Zeitels SM, Hillman RE, Karajanagi SS, Langer RS. Hydrogels for vocal cord and soft tissue augmentation and repair. Google Patents. 2009
75. Chan RW. Measurements of vocal fold tissue viscoelasticity: Approaching the male phonatory frequency range. Journal of the Acoustical Society of America. 2004; 115(6):3161–3170. [PubMed: 15237840]
76. Chan RW, Rodriguez ML. A simple-shear rheometer for linear viscoelastic characterization of vocal fold tissues at phonatory frequencies. Journal of the Acoustical Society of America. 2008; 124(2):1207–1219. [PubMed: 18681608]
77. Shi JH, Guan H, Shi S, Cai WX, Bai XZ, Hu XL, Fang XB, Liu JQ, Tao K, Zhu XX, et al. Protection against TGF-beta 1-induced fibrosis effects of IL-10 on dermal fibroblasts and its potential therapeutics for the reduction of skin scarring. Archives of Dermatological Research. 2013; 305(4):341–352. [PubMed: 23321694]
78. Mast BA, Diegelmann RF, Krummel TM, Cohen I. Scarless wound healing in the mammalian fetus. Surg Gynecol Obstet. 1992; 174(5):441–451. [PubMed: 1570625]
79. King S, Guille J, Thibeault S. Macrophage Phenotype in Acute Porcine Vocal Fold Injuries. Faseb Journal. 2015:29.
80. Vogel C, Marcotte EM. Insights into the regulation of protein abundance from proteomic and transcriptomic analyses. Nature Reviews Genetics. 2012; 13(4):227–232.
81. Ching Y-H, Sutton TL, Pierpont YN, Robson MC, Payne WG. The use of growth factors and other humoral agents to accelerate and enhance burn wound healing. Eplasty. 2011; 11(7):e41. [PubMed: 22084646]
82. Greenhalgh DG. The role of growth factors in wound healing. Journal of Trauma and Acute Care Surgery. 1996; 41(1):159–167.
83. Brancato SK, Albina JE. Wound Macrophages as Key Regulators of Repair Origin, Phenotype, and Function. American Journal of Pathology. 2011; 178(1):19–25. [PubMed: 21224038]
84. Wynn TA, Vannella KM. Macrophages in Tissue Repair, Regeneration, and Fibrosis. Immunity. 2016; 44(3):450–462. [PubMed: 26982353]

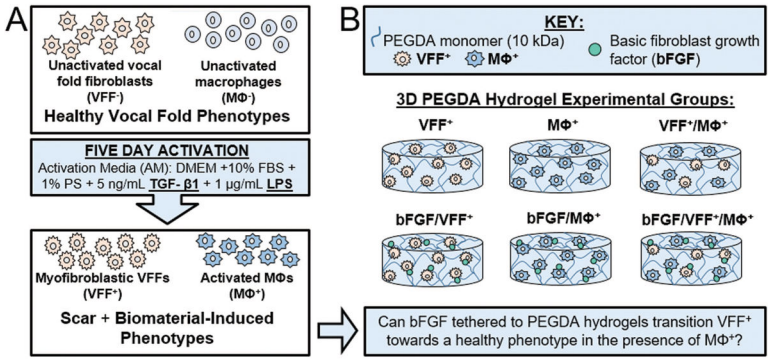

Figure 1.

Overall experimental design for the study. (A) First, scar and biomaterial-induced vocal fold phenotypes (VFF^+ and $M\Phi^+$) were experimentally created through treatment of VFF^- and $M\Phi^-$ with activation media (AM) containing TGF-β1 and LPS for 5 days. (B) Following confirmation of this activation protocol in 2D, more complex 3D studies were performed. The experimental groups analyzed to determine if bFGF tethered to PEGDA hydrogels can transition VFF^+ towards a more normal phenotype in the presence of $M\Phi^+$ are depicted schematically.

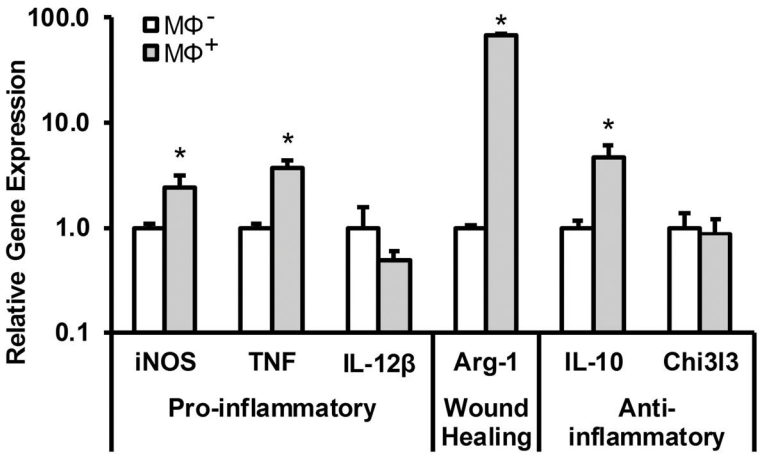

Figure 2.

Gene expression of a panel of markers representing pro-inflammatory, wound healing, or anti-inflammatory phenotypes in macrophages after 5 day activation with LPS/TGF-β1 (MΦ $^{+}$) relative to MΦ $^{-}$. * denotes a significant difference, $p < 0.05$.

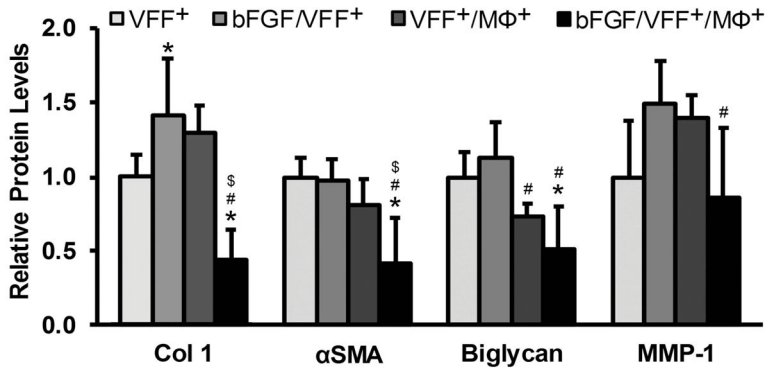

Figure 3.

Relative protein levels of fibrotic tissue markers (Col 1, αSMA and Biglycan) and the anti-fibrotic marker MMP-1 in VFF following 72 h culture in various 3D PEGDA hydrogel experimental groups. *,#,$ denote a significant difference from the VFF^+, bFGF/VFF^+, and $VFF^+/M\Phi^+$ groups, respectively.

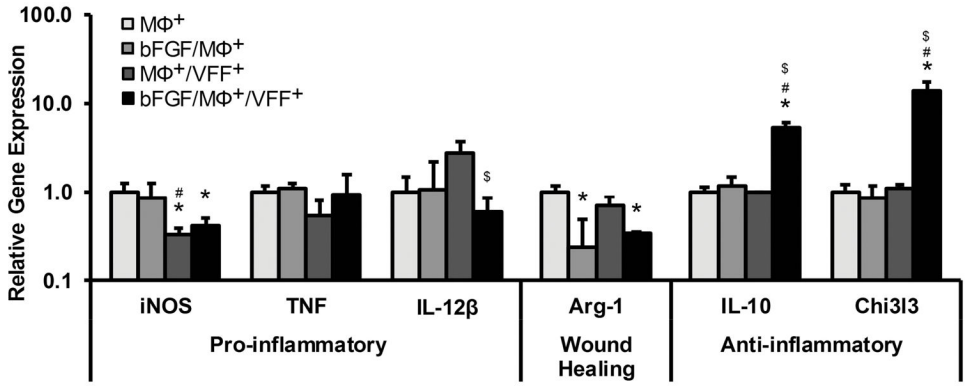

Figure 4.

Relative gene expression of a panel of markers representing pro-inflammatory, wound healing, or anti-inflammatory phenotypes in MΦ following 72 h culture in various 3D PEGDA hydrogel experimental groups. *,#,$ denote a significant difference from the $M\Phi^+$, $bFGF/M\Phi^+$, and $M\Phi^+/VFF^+$ groups, respectively.

Table 1

Primer sequences used for qRT-PCR analysis of genes associated with macrophage polarization.

Macrophage Function	Gene Marker	Primer sequence Forward (F), Reverse (R)	Melting Temp (°C)
Classically Activated	Inducible nitric oxide synthase (iNOS)	F: GAGACAGGGAAGTCTGAAGCAC R: CCAGCAGTAGTTGCTCCTCTTC	82.4
	Tumor necrosis factor (TNF)	F:GGTGCCTATGTCTCAGCCTCTT R:GCCATAGAACTGATGAGAGGGAG	83.6
	Interleukin-12 beta (IL-12β)	F:TTGAACTGGCGTTGGAAGCACG R:CCACCTGTGAGTTCTTCAAAGGC	79.2
	Interleukin-1 beta (IL-1β)	F:TGGACCTTCCAGGATGAGGACA R:GTTCATCTCGGAGCCTGTAGTG	81.8
Wound Healing	Arginase-1 (Arg-1)	F: GCCTTTCAAGGAGCTGTGCAAAA R: GAGCAAAAGGCTGAGCTTCAAGC	81.9
	Vascular endothelial growth factor (VEGF)	F: CTGCTGTAACGATGAAGCCCTG R: GCTGTAGGAAGCTCATCTCTCC	85.0
Anti-Inflammatory	Interleukin-10 (IL-10)	F: CCACAGACCTTCCAGGAGAATG R: GTGCAGTTCAGTGATCGTACAGG	82.9
	Chitinase 3-like 3 (Chi3l3)	F: CTCTTCTGCCTGCTGCACTTTG R: ATGGGCTACAGGCTTGTCACTC	79.0
Reference	Glyceraldehyde 3-phosphate dehydrogenase (GAPDH)	F: GCAGTGGCAAAGTGGAGATT R: CGCTCCTGGAAGATGGTGAT	83.3